The Hückel Molecular Orbital Theory And Its Extensions.

PUNIT K. JHA[1,*]

[1] *The University of Illinois at Urbana-Champaign*
[*] *Corresponding author: punit2@illinois.edu*

Compiled April 30, 2017

The Hückel method or the Hückel molecular orbital method was proposed by Erich Hückel in 1930. In this method, linear combination of atomic orbitals molecular orbitals (LCAO MO) is used for the determination of energies of molecular orbitals of π electrons in planar conjugated hydrocarbon systems, such as ethene, benzene etc. This method forms the theoretical basis for Hückel rule, which estimates whether a planar ring molecule will have aromatic properties or not. This theory only includes the π electron molecular orbitals and neglects the sigma electrons since the π electrons determine the general properties of planar conjugated systems. In this project we develop a C++ program to:
1. Analyze the photoelectron spectra of polycyclic aromatic hydrocarbon (PAH).
2. Study the one dimensional π band structure of polyacetylene and single-wall carbon nanotubes (SWNT).
3. Analyze the two-dimensional π band structure of graphene.
4. Use the Su-Schrieffer-Heeger Model to see the effect of bond-length variation on the energy bands and total energy of benzene, benzene cation and 1, 3, 5, 7-cyclooctatetraene (COTE), and show the origins of the Jahn-Teller distortion (enhancement to the Hückel method has been used in case of COTE).
5. Use the Su-Schrieffer-Heeger model to see the effect of bond-length variation on the energy bands and total energy of polyacetylene and discuss its effects with respect to the Peierls theorem.

INTRODUCTION

The vast majority of polyatomic molecules can be thought of as consisting of a collection of 2-electron bonds between pairs of atoms. The picture of a σ and π-bonding and anti-bonding orbitals for a molecule like CO_2 can be carried over to give a qualitative starting point for describing, say for instance, a C= O bond in acetone. This picture is extremely useful in dealing with conjugated systems - that is, molecules that contain a series of alternating double/single bonds in their Lewis structure like *trans*-polyacetylene as shown in Figure (1).

A common way to represent the electronic structure of *trans*-polyacetylene is by using either the 2 mesomeric Lewis structures represented in Figure (2) (a) and (b) or the average structure of Figure (2) (c). In the latter, all the C – C bonds are equivalent and the dotted lines are used to represent additional C – C bonding with a bond order of 1/2 per C – C pair, delocalised all along the chain.

Conjugated molecules, often tend to be planar and hence all the atoms in the molecules can be assumed to lie in the same plane, say the x-y plane. Which means that the molecule will have a reflection symmetry about the z-axis. So we have reflection symmetry about x and y and this gives rise to π_y orbitals that are anti-symmetric with respect to reflection and the σ orbitals that are symmetric to reflection about the y axis. These π_y orbitals will be an linear combination of the p_y orbitals on each of the carbon atoms.

In general, since the π orbitals are the highest occupied or-

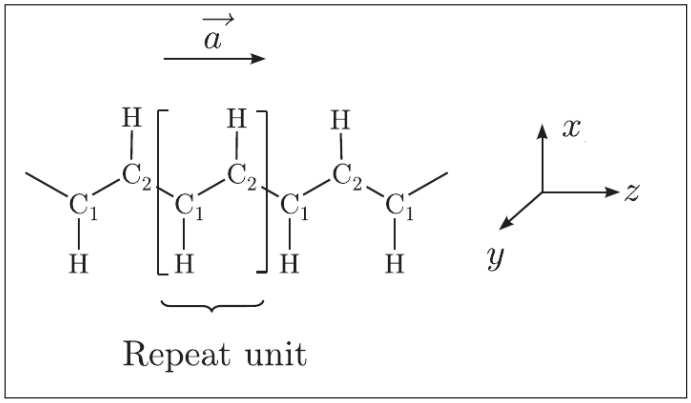

Fig. 1. Structure of *trans*-polyacetylene chain : the system is generated by a repeat unit containing 2 carbon and 2 hydrogen atoms and a repeat vector $\vec{a}$.

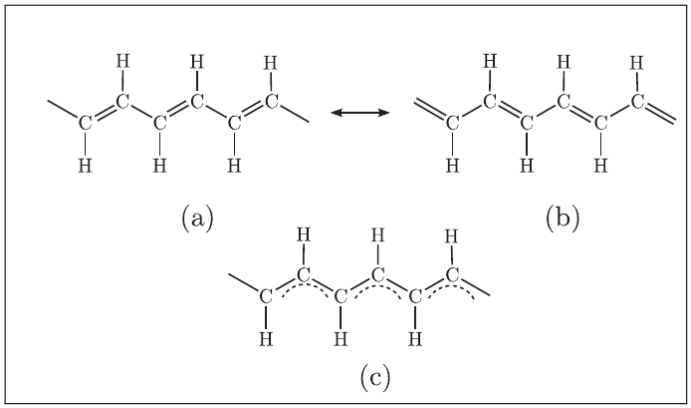

Fig. 2. (a)-(b) Mesomeric Lewis structures for *trans*-polyacetylene; (c) average structure of *trans*-polyacetylene.

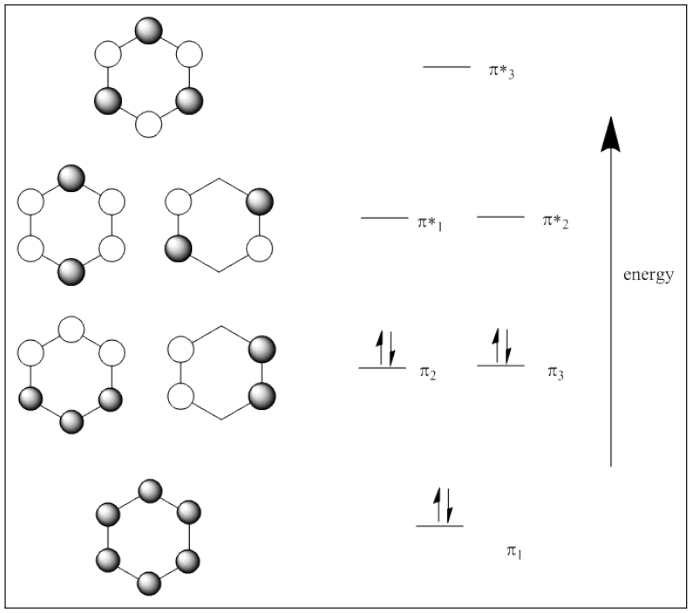

Fig. 3. The eigenvalues of the **H** matrix for benzene. The lowest and the highest energies are non-degenerate while the second and the third energy levels are degenerate. The figure also depicts the filling up of 6 π electrons in benzene.

bitals and the σ bonds are more strongly bonded – it makes sense to talk only the π bond when talking about bond formation and breaking as implied by the resonance structures shown in Figure (2). This is a basic approximation of the very simple Hückel approach.

Hückel Theory

As always we start with the time-dependent Schrödinger equation,

$$\hat{H}\Psi = E\Psi \tag{1}$$

where $\hat{H}$ is the Hamiltonian and Ψ is the wavefunction and E is the total energy. The next step is to expand the wave function as linear combination of the basis functions:

$$\Psi = \sum_{i=i..n} c_i \chi_i \tag{2}$$

Here the c_i are the expansion coefficients and χ_i are the basis functions, and n the total number of basis functions used. By substituting, Equation (2) into Equation (1) and applying the variational theorem, we derive the Schrödinger equation in secular from as shown below:

$$det[\mathbf{H} - E\mathbf{S}] = 0. \tag{3}$$

Where **H** is the matrix whose elements – called the energy integral– are given by :

$$H_{ij} = \int \chi_i^* \hat{H} \chi_j d\tau \tag{4}$$

and **S** is the matrix whose elements called the overlap integrals--are given by,

$$S_{ij} = \int \chi_i^* \chi_j d\tau \tag{5}$$

In the Hückel approach we choose the basis function to be the atomic orbitals. So we choose the p_y orbitals in our case and we apply the first approximation that the orbitals are orthonormal. Which reduces the **S** matrix to a identity matrix– and our generalized eigenvalue problem is reduced to a normal eigenvalues problem as shown in Equation (1). The second approximation is to assume that any Hamiltonian integrals vanish if they involve atoms i, j that are not the nearest neighbors. This makes sense as the p_y orbitals are far apart and have a very limited partial overlap. Also the diagonal terms are the same since these involve the average energy of an electron in a carbon p_y orbital.

$$H_{ii} = \int p_y^i \hat{H} p_y^i d\tau = \alpha \tag{6}$$

α is generally called the on-site energy. For any two nearest neighbors, the matrix element is also assumed to be constant.

$$H_{ij} = \int p_y^i \hat{H} p_y^j d\tau = \beta \tag{7}$$

β is called the resonance integral and this assumption holds good as long as the C – C bond is the remains the same.
After the above assumptions as made the **H** matrix for a

molecule say -benzene with 6 carbon atoms looks something like:

$$\mathbf{H} = \begin{bmatrix} \alpha & \beta & 0 & 0 & 0 & \beta \\ \beta & \alpha & \beta & 0 & 0 & 0 \\ 0 & \beta & \alpha & \beta & 0 & 0 \\ 0 & 0 & \beta & \alpha & \beta & 0 \\ 0 & 0 & 0 & \beta & \alpha & \beta \\ \beta & 0 & 0 & 0 & \beta & \alpha \end{bmatrix} \tag{8}$$

Solving, i.e, diagonalizing the **H** matrix, we find 4 distinct energies as shown in the Figure (3). Again, since there are 3 π bonds in benzene we can fill the 6 electrons by doubly occupying the first three molecular orbitals as shown in the Figure (3). The Hückel energy of benzene is then calculated as:

$$E = 2E_1 + 2E_2 + 2E_3 = 6\alpha + 8\beta \tag{9}$$

The eigenvectors corresponding to these energy states can be obtained and they are:

$$\mathbf{c}^1 = \frac{1}{\sqrt{6}} \begin{bmatrix} +1 \\ +1 \\ +1 \\ +1 \\ +1 \\ +1 \end{bmatrix} \mathbf{c}^2 = \frac{1}{\sqrt{12}} \begin{bmatrix} +1 \\ +2 \\ +1 \\ -1 \\ -2 \\ -1 \end{bmatrix} \mathbf{c}^3 = \frac{1}{\sqrt{4}} \begin{bmatrix} +1 \\ 0 \\ -1 \\ -1 \\ 0 \\ +1 \end{bmatrix} \tag{10}$$

$$\mathbf{c}^4 = \frac{1}{\sqrt{4}} \begin{bmatrix} +1 \\ 0 \\ -1 \\ +1 \\ 0 \\ -1 \end{bmatrix} \mathbf{c}^5 = \frac{1}{\sqrt{12}} \begin{bmatrix} +1 \\ -2 \\ +1 \\ +1 \\ -2 \\ +1 \end{bmatrix} \mathbf{c}^6 = \frac{1}{\sqrt{6}} \begin{bmatrix} +1 \\ -1 \\ +1 \\ -1 \\ +1 \\ -1 \end{bmatrix} \tag{11}$$

The energy calculated above presents an interesting result – it predicts that benzene is more stable than a normal 3 double bond system. If we carry out a Hückel theory calculation for ethylene molecule we find that a single ethylene molecule has an energy of:

$$E_{C=C} = 2\alpha + 2\beta \tag{12}$$

Thus, for three double bonds this becomes

$$E = 3 \times E_{C=C} = 6\alpha + 6\beta \tag{13}$$

This is off by 2β. And since β is a measure of the strength of the bonding interaction as a result of the overlap of orbitals i and j orbitals - it is negative for constructive overlap of orbitals - so the π electrons in benzene are more stable than a collection of three double bonds. This is called *aromatic stabilization*. Now we analyze the bond order. In the Hückel theory the bond order can be defined as:

$$O_{ij} = \sum_{\mu=1}^{occ} = c_i^\mu c_j^\mu \tag{14}$$

This definition incorporates the idea that if molecular orbital μ has a bond between the ith and jth carbons, then the coefficients of the molecular orbital on those carbons should both have the same sign (e.g we have $p_y^i + p_y^j$), similarly if its an anti-bonding orbital then the coefficients have the opposite sign (e.g we have $p_y^i - p_y^j$). The expression above reflects that :

$$c_i^\mu c_j^\mu > 0 \textbf{ if } c_i^\mu c_j^\mu \textbf{ have the same sign} \tag{15}$$

$$c_i^\mu c_j^\mu < 0 \textbf{ if } c_i^\mu c_j^\mu \textbf{ have the opposite sign} \tag{16}$$

Equation (14) gives a positive contribution for bonding orbitals and a negative contribution for anti-bonding. A doubly occupied orbital appears twice in the summation. The summation over the occupied orbitals sums up the bonding or anti-bonding contributions from all the occupied molecular orbitals for the particular i-j pair of carbons to give the total bond order. Applying the Equation (14) to the C_1 and C_2 of the benzene molecule we get:

$$\begin{aligned} O_{12} =& 2c_1^{\mu=1}c_2^{\mu=1} + 2c_1^{\mu=2}c_2^{\mu=2} + 2c_1^{\mu=3}c_2^{\mu=3} \\ &= 2\left(\frac{+1}{\sqrt{6}}\right)\left(\frac{+1}{\sqrt{6}}\right) + 2\left(\frac{+1}{\sqrt{12}}\right)\left(\frac{+1}{\sqrt{12}}\right) + \\ &2\left(\frac{+1}{\sqrt{4}}\right)\left(\frac{0}{\sqrt{4}}\right) \\ &= 2 \times \frac{1}{6} + 2 \times \frac{2}{12} \\ &= \frac{2}{3} \end{aligned} \tag{17}$$

Thus, the C_1 and C_2 of the benzene share $\frac{2}{3}$ of a π bond. Repeating the procedure for each of the $C-C$ atoms we find the same bond order for all of them (taking note of the fact that we have omitted the σ orbital contributions). This is again an interesting results, since for a double bond we have a bond order of $\frac{1}{2}$ for each bond C – C π-bond rather than $\frac{2}{3}$. The additional $\frac{1}{6}$ of a bond per carbon comes directly from the aromatic stabilization – as the molecule is more stable than a three isolated π bonds by 2β. This higher bond order results in a shorter C – C bond length in benzene as compared to non-aromatic conjugated systems.

The procedure for constructing the Hückel Hamiltonian was computationally implemented in the C++ programming language for benzene, anthracene, hexacene, and peropyrene. The input connectivity files for these molecules are attached with the email and the resulting orbital energies assuming $\alpha = 0$, $\beta = -1$ and $\alpha = 5.94\ eV$, $\beta = 2.94\ eV$ are shown in Table (1) and (2) .

Table 1. π **Orbital Energies**

Molecule	$\alpha = 0, \beta = -1$	$\alpha = -5.94\ eV, \beta = -2.94\ eV$
Benzene	-2.0000	0.0600
	-1.0000	3.0000
	-1.0000	3.0000
	$+1.0000$	8.8800
	$+1.0000$	8.8800
	$+2.0000$	11.820
Anthracene	-2.4142	-1.1578
	-2.0000	0.0600
	-1.4142	1.7822
	-1.4142	1.7822
	-1.0000	3.0000
	-1.0000	3.0000
	-0.4142	4.7222
	$+0.4142$	7.1578
	$+1.0000$	8.8800
	$+1.0000$	8.8800
	$+1.4142$	10.0978
	$+1.4142$	10.0978
	$+2.0000$	11.8200
	$+2.4142$	13.0378
Hexacene	-2.5074	-1.4316
	-2.3489	-0.9658
	-2.0994	-0.2322
	-1.7866	0.6873
	-1.5349	1.4274
	-1.4701	1.6179
	-1.3519	1.9653
	-1.2392	2.2967
	-1.0591	2.8261
	-1.0000	3.0000
	-0.6913	3.9075
	-0.3372	4.9485
	-0.0485	5.7974
	0.0485	6.0826
	0.3372	6.9315
	0.6913	7.9725
	1.0000	8.8800
	1.0591	9.0539
	1.2392	9.5833
	1.3519	9.9147
	1.4701	10.2621

Table 2. π **Orbital Energies**

Molecule	$\alpha = 0, \beta = -1$	$\alpha = -5.94\ eV, \beta = -2.94\ eV$
Hexacene	1.5349	10.4526
	1.7866	11.1927
	2.0994	12.1122
	2.3489	12.8458
	2.5074	13.3116
Peropyrene	-2.6431	-1.7227
	-2.3876	-0.7492
	-2.0000	0.1978
	-1.9190	0.3482
	-1.6825	0.8478
	-1.5435	1.3590
	-1.3097	1.9114
	-1.1159	2.7540
	-1.0000	3.0000
	-1.0000	3.0000
	-0.8308	3.4653
	-0.8280	4.2493
	-0.2846	5.1144
	0.2846	6.7656
	0.8280	7.6307
	0.8308	8.4147
	1.0000	8.8800
	1.0000	8.8800
	1.1159	9.1260
	1.3097	9.9686
	1.5435	10.5210
	1.6825	11.0322
	1.9190	11.5318
	2.0000	11.6822
	2.3876	12.6292
	2.6431	13.6027

FREE-ELECTRON MODEL

A system behaves as a metal if it has valence orbitals not tightly bound to the nuclei. A metal can be viewed as series of electrons which move freely over a network of fixed cations. The potential felt by electron is assumed to be nil in the solid but equal to a positive and large value ($+V_0$) outside. The electron is thus confined to the metallic piece and the different forced felt by the electron in the metal (attractive or repulsive) are neglected. Being interested in collective properties of the bulk material in general, we impose a boundary condition so that the effects at the borders are neglected. We then determine the wavefunctions

describing the behavior of an electron in this ideal metal.

1D System and Its Eigenvectors

Consider an electron constrained to move through a linear segment of length L. Writing the Schrödinger equation for this 1-D system we have :

$$-\frac{\hbar^2}{2m}\frac{d^2\Psi(x)}{dx^2}+V(x)\Psi(x)=E\Psi(x) \quad (18)$$

Where $\Psi(x)$ is the wavefunction describing an electron at point M with coordinate x, E is the energy of the electron, $V(x)$ is the potential at the M point. In the free electron model the potential is nil for any point of the system therefore the above equation becomes :

$$\forall x \in \ ]-\frac{L}{2},\frac{L}{2}] \quad -\frac{\hbar^2}{2m}\frac{d^2\Psi(x)}{dx^2}=E\Psi(x) \quad (19)$$

for which the general solution is the interval is given by] -L/2, L/2] is given by :

$$\Psi(x)=C_+exp(ikx)+C_-exp(-ikx) \quad (20)$$

where $k=\frac{\sqrt{2mE}}{\hbar}$ and E ≥ 0 . C_+ and C_- are the two constants such that the wavefunction is not nil in] -L/2, L/2] interval. We also obtain a linear combination of two waves associated with opposite wave vectors $\vec{k}$ with projections k and $-k$ on the x axis.

Born-von Karmen boundary Condition

Now, we impose boundary conditions to be able to characterize the wavefunction for any point M. We adopt a approach which makes equivalent the linear system and the cyclic system with perimeter L in the interval +L/2 and -L/2, as shown in Figure (4). The point M in the linear representation is equivalent to the point M characterized by the angle ϕ_M in the cyclic representation:

$$\phi_M=\frac{x}{L}2\pi; \quad \phi_M \in \ ]-\pi,\pi] \quad (21)$$

The wavefunction of the electron in the cyclic representation as well as its derivative must verify the following boundary conditions:

$$\Psi(-\pi)=\Psi(\pi) \quad and \quad \Psi'(-\pi)=-\Psi'(\pi) \quad (22)$$

where Ψ' is the derivative of Ψ. Since the linear and the cyclic systems are equivalent, the Ψ of the linear system must satisfy the following periodicity condition:

$$\Psi\Big(-\frac{L}{2}\Big)=\Psi\Big(\frac{L}{2}\Big) \quad and \quad \Psi'\Big(-\frac{L}{2}\Big)=-\Psi'\Big(\frac{L}{2}\Big) \quad (23)$$

We retain only those eigenstates that satisfy the above periodicity conditions in Equation (23), in other words:

$$C_+exp\Big(-ik\frac{L}{2}\Big)+C_-exp\Big(ik\frac{L}{2}\Big)=C_+exp\Big(ik\frac{L}{2}\Big)+C_-exp\Big(-ik\frac{L}{2}\Big) \quad (24)$$

$$kC_+exp\Big(-ik\frac{L}{2}\Big)-kC_-exp\Big(ik\frac{L}{2}\Big)=kC_+exp\Big(ik\frac{L}{2}\Big)-C_-exp\Big(-ik\frac{L}{2}\Big) \quad (25)$$

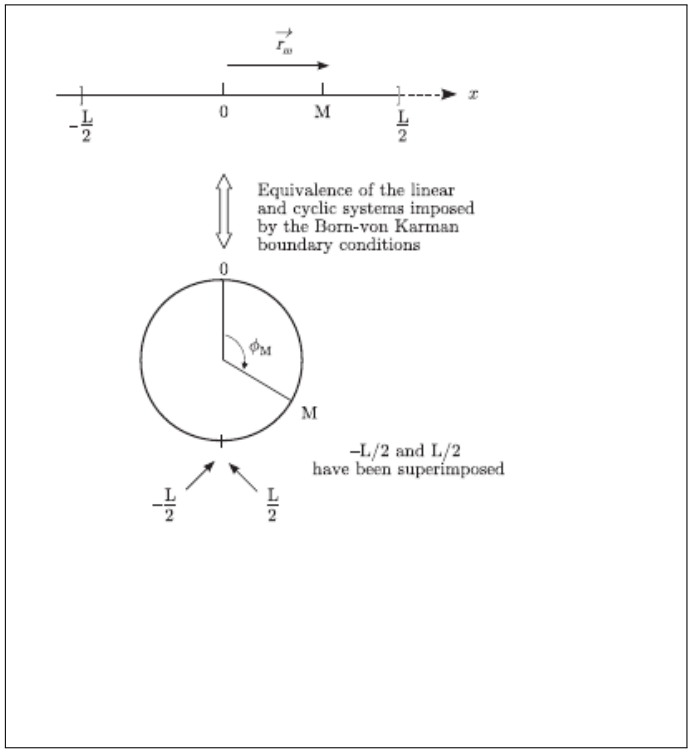

Fig. 4. Equivalence between a very large linear system and a cyclic system

k-space

Rearranging the above equations we get:

$$2isin\Big(k\frac{L}{2}\Big)(C_+-C_-)=0 \quad (26)$$

$$2iksin\Big(k\frac{L}{2}\Big)(C_++C_-)=0; \quad (27)$$

However the quantities (C_+-C_-) and (C_++C_-) are not simultaneously nil except if the C_+ and C_- constant are both nil, which is not possible as shown in Equation (20). This means that the term $sin(k\frac{L}{2})$ must be nil.

$$sin\Big(k\frac{L}{2}\Big)=0 \Rightarrow k\frac{L}{2}=n\pi \quad if \ n \ is \ an \ integer \quad (28)$$

As a result, k is quantized and must be a multiple of $\frac{2\pi}{L}$. The solutions verifying the Schrödinger equation for this 1-D system Equation (18) as well as the boundary conditions of Equation (22) are labelled $\Psi_k(x)$ and are given by :

$$\Psi_k(x)=Nexp(ikx) \text{ where N is a normalization constant} \quad (29)$$

$$\text{with} \quad k=\frac{2n\pi}{L} \quad (30)$$

In other word, k may adopt the values $0, \pm\frac{2\pi}{L}, \pm\frac{4\pi}{L}$...

Any linear combination of the degenerate wavefunctions $\Psi_k(x)$ and $\Psi_{-k}(x)$ is also the solution of the Schrödinger equation (18) as well as obeys the boundary conditions of Equation (22), because no restriction is imposed on the C_+ and C_- coefficients.

As shown in Equation (20), the quantization of k also imposes quantizations on the energy. We label $E(k)$ the energy associated with the waves $\Psi_k(x)$ and $\Psi_{-k}(x)$:

$$E(k) = \frac{(\hbar k)^2}{2m} \tag{31}$$

These functions may be written in he following vectorial notations:

$$\Psi_{\vec{k}}(\vec{r}_m) = Nexp(i\vec{k}.\vec{r}_m) \text{ if } \vec{k} = k\vec{i}_x \text{ and} \vec{r}_m = x\vec{i}_x \tag{32}$$

The wave function $\Psi_{\vec{k}}(\vec{r}_m)$ is the wave associated with an electron with a momentum $\vec{p}$ equal to $\hbar\vec{k}$. We note that the states $\Psi_{\vec{k}}(\vec{r}_m)$ and $\Psi_{-\vec{k}}(\vec{r}_m)$ are degenerate.

Normalizing $\Psi_{\vec{k}}(\vec{r}_m)$ in the]-L/2, L/2] interval we get $N = \sqrt{\frac{1}{L}}$:

$$\Psi_{\vec{k}}(x) = \sqrt{\frac{1}{L}}exp(ikx) = \sqrt{\frac{1}{L}}exp(i\vec{k}\vec{r}_m) \tag{33}$$

The allowed levels of $k = 0, \pm\frac{2\pi}{L}, \pm\frac{4\pi}{L}$... can be be represented on an axis as shown in Figure (5).

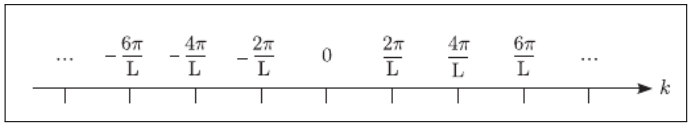

Fig. 5. Allowed values of k

From the discussion above we know that only a certain values of k are allowed. The Brillouin zone is the region of allowed k values of the system.

Fermi Level

Since we neglected the electron-electron repulsions, electrons fill the lowest energy levels, with two electrons per allowed state in the ground state at T=0 K. The Fermi level, ϵ_f is the highest energy level filled in the ground state at T=0 K. This highest filled level is characterized by the $\pm\vec{k}_f$ wave vectors and its energy ϵ_f is given as :

$$\epsilon_f = \frac{(\hbar k_f)^2}{2m} \tag{34}$$

In Figure (6) a system with 7 electrons is shown, these are filled up in the allowed energy levels and the Fermi level - ϵ_f - is shown.

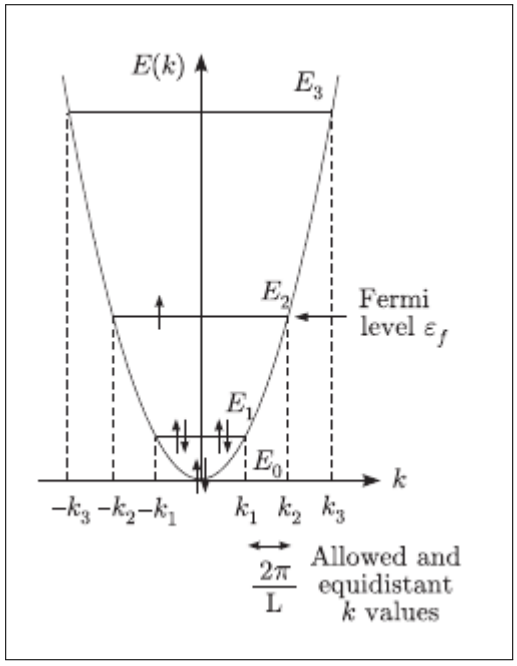

Fig. 6. Allowed energy levels for a 1-D system fulfilling the Born-von Karman boundary conditions. The image is not to scale and the energy levels are drawn far apart from each other. The Fermi level is marked in the image.

The Su-Schrieffer-Heeger (SSH) model

The Su-Schrieffer-Heeger (SSH)[8] model describes the electrons hopping on a chain (1-dimensional lattice) as shown in Figure (7). The chain has N unit cells, each unit cell hosting 2 sites, one on the sublattice A and another on the sublattice B. Interactions among the electrons are neglected, and so the dynamics of each electron is described by a single-particle Hamiltonian, of the form:

$$\hat{H} = v\sum_{m=1}^{N}(|m,B\rangle\langle m,A| + h.c.) + w\sum_{m=1}^{N-1}(|m+1,A\rangle\langle m,B| + h.c.) \tag{35}$$

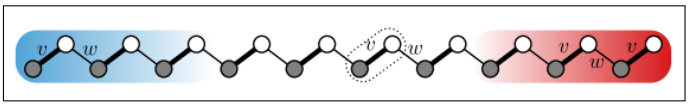

Fig. 7. Geometry of the SSH model.[8] Filled circles are site on the sublattice A and empty ones on B, each hosting a single state. The dotted line shows an unit cell. The intracell hopping is v (thin lines) is different from the intercell hopping w (thick lines). The red and blue colors indicate the edges.

Here $|m,A\rangle$ and $|m,B\rangle$ with $m \in 1,2,...N$ denote the state of the chain where the electron is on unit cell m, in the site on sublattice A, and B respectively. $h.c$ stands for the Hermitian Conjugate terms. The Hamiltonian is spin independent, and thus when acting on a real physical system, e.g., polyacetylene, two copies of the Hamiltonian have to be taken to represent two possibilities of spin orientation.

We analyze the orientation of electrons in and around the ground state of the SSH model at zero temperature and zero

chemical potential, where all the eigenstates of the Hamiltonian are singly occupied. There are N such on site potential terms. This situation called half filling is the characteristic of insulators, such as polyacetylene where each carbon carries one conduction electron. So, we have one particle in a cell. The matrix for the Hamiltonian of the SSH model, based on Equation (35) on a real space basis, for a chain of N=4 unit cells is written as:

$$\mathbf{H} = \begin{bmatrix} 0 & v & 0 & 0 & 0 & 0 & 0 & 0 \\ v & 0 & w & 0 & 0 & 0 & 0 & 0 \\ 0 & w & 0 & v & 0 & 0 & 0 & 0 \\ 0 & 0 & v & 0 & w & 0 & 0 & 0 \\ 0 & 0 & 0 & w & 0 & v & 0 & 0 \\ 0 & 0 & 0 & 0 & v & 0 & w & 0 \\ 0 & 0 & 0 & 0 & 0 & w & 0 & v \\ 0 & 0 & 0 & 0 & 0 & 0 & v & 0 \end{bmatrix} \tag{36}$$

Hückel 1D band structure

The dynamical (k-dependent) Hamiltonian matrix in the Hückel model for the bond alternating structure for *trans*-polyacetylene is given as :

$$\mathbf{H}(k) = \begin{bmatrix} 0 & -0.9 \\ 0 & 0 \end{bmatrix} e^{-ik} + \begin{bmatrix} 0 & -1.1 \\ -1.1 & 0 \end{bmatrix} + \begin{bmatrix} 0 & 0 \\ -0.9 & 0 \end{bmatrix} e^{ik} \tag{37}$$

The eigenvalues of these equations were plotted as a function of k in the Figure (8).

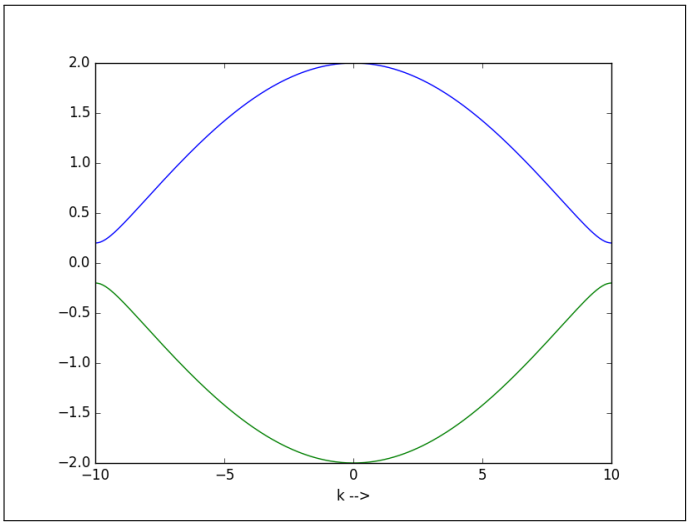

Fig. 8. Eigenvalues as a function of k are energy band gaps and a non-zero fundamental band gap is observed. The cell length was taken to be 1 and the k vector was varied from $+\pi$ to $-\pi$. The points are in the first Brillouin zone.

Trans-polyacetylene becomes metallic with equidistant C-C bond (generally this is not the case due to Peierls distortion as explained in later sections). In the new Hamiltonian, the resonance integral β becomes -1 and the full $\mathbf{H}$ is :

$$\mathbf{H}(k) = \begin{bmatrix} 0 & -1.0 \\ 0 & 0 \end{bmatrix} e^{-ik} + \begin{bmatrix} 0 & -1.0 \\ -1.0 & 0 \end{bmatrix} + \begin{bmatrix} 0 & 0 \\ -1.0 & 0 \end{bmatrix} e^{ik} \tag{38}$$

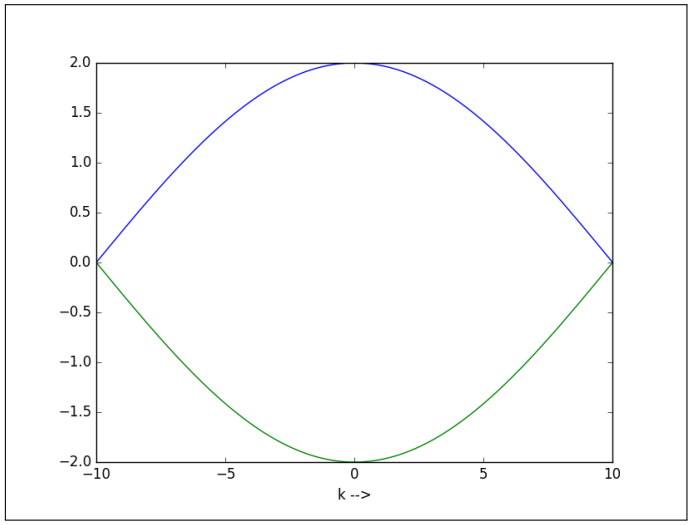

Fig. 9. Eigenvalues as a function of k are energy band gaps and a fundamental band gap is not observed. The cell length was taken to be 1 and the k vector was varied from $+\pi$ to $-\pi$. The points are in the first Brillouin zone.

Extending the codes developed above, to single walled carbon nanotube (SWNT), which has 4 carbons on the circumference, we get the plot of eigenvalues as a function of k (which are the energy bands) shown in Figure (10). The new Hamiltonian matrix takes the form as shown below.

$$\mathbf{H}(k) = \begin{bmatrix} 0 & -1 & 0 & 0 \\ 0 & 0 & -1 & 0 \\ 0 & 0 & 0 & -1 \\ -1 & 0 & 0 & 0 \end{bmatrix} e^{-ik} + \begin{bmatrix} 0 & 0 & 0 & -1 \\ 0 & 0 & -1 & 0 \\ 0 & -1 & 0 & 0 \\ -1 & 0 & 0 & 0 \end{bmatrix} + \begin{bmatrix} 0 & 0 & 0 & -1 \\ -1 & 0 & 0 & 0 \\ 0 & -1 & 0 & 0 \\ 0 & 0 & -1 & 0 \end{bmatrix} e^{ik} \tag{39}$$

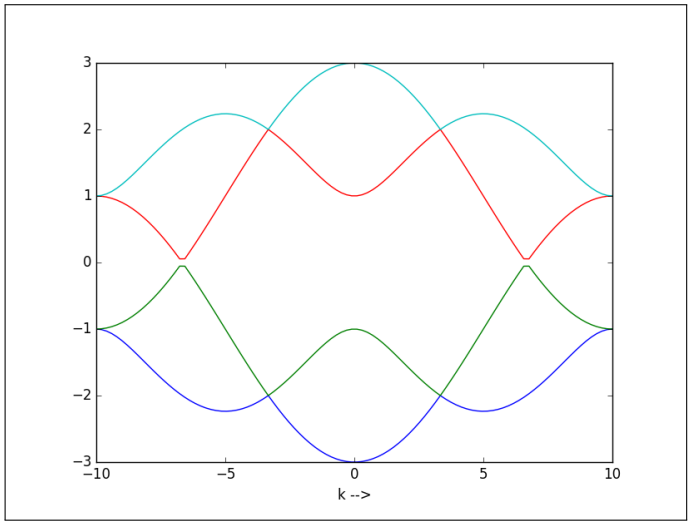

Fig. 10. Plot of eigenvalues as a function of k for a SWNT which has 4 carbons on the circumference. The k vector was varied from $+\pi$ to $-\pi$. The points are in the first Brillouin zone.

Then we apply our codes to a SWNT which has 10 carbons on its circumference and we get the plot shown in Figure (11).

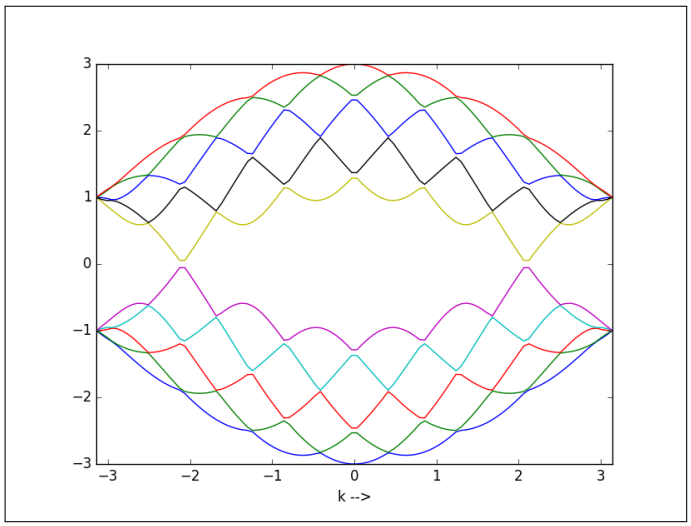

Fig. 11. Plot of eigenvalues as a function of k for a SWNT which has 10 carbons on the circumference. The k vector was varied from $+\pi$ to $-\pi$. The points are in the first Brillouin zone.

Hückel 2D band structure

We now extend the codes written for the 1D Hückel band structure to a 2D system, say graphene. The dynamical Hamiltonian matrix in the Hückel model and the corresponding energy bands are now functions of two k vectors. The Hamiltonian is :

$$\mathbf{H}(k) = \begin{bmatrix} 0 & 0 \\ -1.0 & 0 \end{bmatrix} e^{-ik_1} + \begin{bmatrix} 0 & -1.0 \\ 0 & 0 \end{bmatrix} e^{-ik_2} + \begin{bmatrix} 0 & -1.0 \\ -1.0 & 0 \end{bmatrix} + \begin{bmatrix} 0 & -1.0 \\ 0 & 0 \end{bmatrix} e^{ik_1} + \begin{bmatrix} 0 & 0 \\ -1.0 & 0 \end{bmatrix} + e^{ik_2} \tag{40}$$

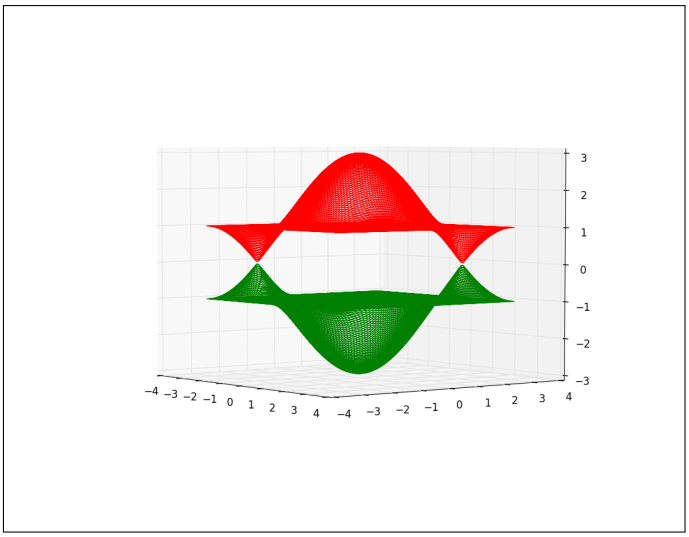

Fig. 12. The valence and conduction bands of a graphene sheet in 2D which depicts pointwise degeneracy. Both the k_1 vector and k_2 vectors were varied from $+\pi$ to $-\pi$

Jahn-Teller Theorem

The Jahn-Teller theorem states that any non-linear molecular system in a degenerate electronic state will be unstable and will undergo distortion to form a system of lower symmetry and lower energy thereby removing the degeneracy. The Jahn-Teller Effect, governed by the Jahn-Teller Theorem, is a phenomenon in which non-linear molecules are stabilized via symmetric geometric distortions along one of their vibrational axes.The theorem does not predict the type of distortion but says that this distortion will lower the complex's symmetry, energy, and degeneracy. The phenomenon exclusively affects systems with electronic degeneracy, and it primarily affects systems with an odd number of electrons.

Using the Su-Schrieffer-Heeger model we study the effect of bond-length variations on the π and σ energies of benzene and benzene cation. The SSH Hamiltonian as a function of change in resonance integral because of bond-length variation becomes:

$$\mathbf{H}(\Delta) = \begin{bmatrix} 0 & -1+\Delta & 0 & 0 & 0 & -1+\Delta \\ -1+\Delta & 0 & -1-2\Delta & 0 & 0 & 0 \\ 0 & -1-2\Delta & 0 & -1+\Delta & 0 & 0 \\ 0 & 0 & -1+\Delta & 0 & -1+\Delta & 0 \\ 0 & 0 & 0 & -1+\Delta & 0 & -1-2\Delta \\ -1+\Delta & 0 & 0 & 0 & -1-2\Delta & 0 \end{bmatrix} \tag{41}$$

The total energy of benzene is given as:

$$E(\Delta) = 2e_1 + 2e_2 + 2e_3 + \frac{1}{2}k(\Delta^2 + \Delta^2 + \Delta^2 + \Delta^2 + 4\Delta^2 + 4\Delta^2) \quad \textbf{(42)}$$

where Δ is the change in resonance integral because of bond-length variation, e_1, e_2 and e_3 are the three lowest-lying eigenvalues of $\mathbf{H(\Delta)}$, and k is the force constant of the σ bond. To model the benzene cation, the coefficient multiplying e_3 is taken to be 1 since there are only 7 electrons in the cation of benzene. The plots that were obtained are shown in Figure (14)

We observe that as Δ increases/decreases the symmetry of benzene D_{6h} is retained while the symmetry of benzene cation is changed from D_{6h} to either a threefold D_{3h} symmetry in which the planar structure is maintained or to C_{3v} chair like structure similar to cyclohexane or an in-plane symmetry reduction to D_{2h} is also possible as described elsewhere [9]. The cause of this change in symmetry is the Jahn-Teller coupling that accompanies electronic degeneracy.

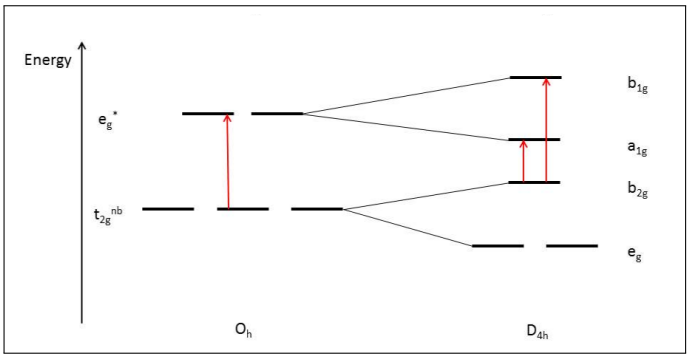

Fig. 13. The energy levels of e_g and t_{2g} orbitals of octahedral complexes, alongside their distorted energy levels. These distortions are caused by the Jahn-Teller Effect.

Deriving the origins of Jahn-Teller distortion from enhanced Hückel Theory (HT)

Equations (1)-(7) represent a standard protocol for carrying out the H*ü*ckel calculations and assuming a particular value of the resonance integral β and energy integral α from experiments render it a semi-empirical flavor. Its not particularly useful for predicting the molecular geometric structure and it is therefore not reliable in predicting the molecular potential energy curve. We now aim to extend the H*ü*ckel theory (HT) and enhance it such that it can predict the molecular potential energy curve and hence, show the origin of the Jahn-Teller distortion[2] [3] in 1, 3, 5, 7-cyclooctatetraene (COTE). This procedure has been described in detail by Sohlberg *et. al* [1]. COTE spontaneously distorts into from a perfect octagon whereas benzene will not distort from a perfect hexagon. The required enhancement is accomplished through the application of Pauli and Aufbau's Principle together with the Hund's rule and the use of Slater's rule for determining the nuclear screening by core electrons.

To get a molecular potential energy curve we must have the sum of electronic total energy and the nuclear-nuclear repulsion energy. First, we produce a total many-electron energy, instead of simply a set of one-electron orbital energies. Secondly, the nuclear-nuclear energy is accounted for.

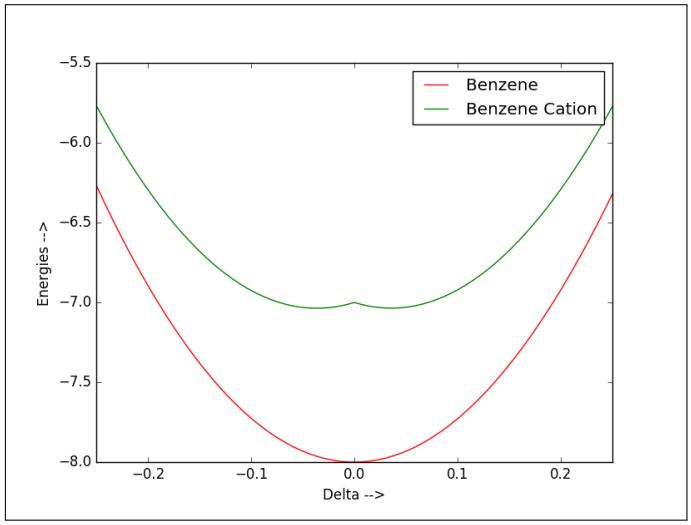

Fig. 14. The plot of benzene and benzene cation as function of symmetry breaking geometry change. Symmetry of benzene D_{6h} is retained while the symmetry of benzene cation is changed from D_{6h} to either D_{3h} symmetry or to C_{3v} chair like structure or to D_{2h} as described elsewhere [9]. The points are in the first Brillouin zone.

Using the Pauli and Aufbau principles together with Hund's rule we assume that each of the n molecular orbitals has an occupancy of 2, 1, or 0 electrons and accordingly the total electronic energy is given by:

$$E_e^k = \sum_{i=1\ldots n} p_i^k E_i \quad \textbf{(43)}$$

where E_e^k is the many-electron energy of the kth electronic state, E_i is the energy of the ith molecular orbital and p_i^k is the occupancy of the ith molecular orbital in the kth state. This approximation assumes that the many-electron wave function is a product of one-electron wave functions and that it does not satisfy the antisymmetry property–a hartree product.

The Hückel Theory (**HT**) is a valence-electron only theory and does not treat the core-electrons. Using the Slater rules we approximate the numerical values for the effective nuclear charge experienced by each electron in a many-electron atom. The effective charge Z^{eff} is given by,

$$Z^{eff} = Z - s \quad \textbf{(44)}$$

where Z is the true nuclear charge and s is the total shielding. The shielding constants are calculated by grouping electrons by principal quantum number n and azimuthal quantum number l. The shielding constant s for each group is given by the sum of following contributions:

- 0.35 for each other electron with the same n and l,
- 0.85 for each other electron with the same n but smaller l and,
- 1 for each other electron with smaller n.

The analogue of nuclear repulsion energy for the HT, the "atomic core repulsion energy " is given as :

$$V_{nn} = \sum_{\alpha>\beta} \frac{Z_\alpha^{eff} Z_\beta^{eff}}{R_{\alpha\beta}} \quad \textbf{(45)}$$

where the Greek letter subscripts run over all atoms in the molecule. The potential energy surface for the kth electronic state (E_k^{tot}) of the molecule is then given by:

$$E_k^{tot} = E_e^k + V_{nn} \tag{46}$$

We note that both E_e^k and V_{nn} depend on the relative spatial position of the constituent atoms in the molecule, that is, the molecule's geometry, so that E_k^{tot} represents an electronic state energy. To apply this procedure to COTE and benzene we observe that they are perfect polygon to begin with (hexagon D_{6h} *symmetry* in the case of benzene and octagon D_{8h} *symmetry* in the case of COTE) that lies in the xy plane. Each bond is taken to be of length R = 2.63 b. (2.63 b = 1.39 Å= 1.39 $\times$ 10^{-10} m).

The distortion of COTE from a perfect octagon, which has D_{8h} *symmetry*, to the lower symmetry D_{4h} *symmetry* structure, which represents alternating single and double bonds along the backbone of the octagon can be represented in terms of the distortion parameter w with the units of length -*bohr*. With the increase in w the bonded atoms alternatively have separation $R - w$ and $R + w$. Our goal is to determine the functional dependence of the ground-state energy on w.

We select the basis set consisting $2p_z$ orbitals (since only the π bonding structure of the molecule is treated in HT) for calculation of the **H** and **S** matrix elements. The overlap between two parallel p_z orbitals to form π structure is given as :

$$s_{(2p\pi-2p\pi)} = \left(1 + \zeta R + \frac{2\zeta^2 R^2}{5} + \frac{\zeta^3 R^3}{15}\right) exp\,(-\zeta R) \tag{47}$$

Here, ζ is the orbital exponent which is taken to be 1.5679 for a carbon $2p_z$ orbital and R is the separation between the two orbital centers. To be able to use the Equation (47) to compute all the elements of the **S** matrix, all the atom-atom distances must be calculated.

To analyze the dependence of the ground-state energy on the distortion parameter w, these atomic distances must be calculated as a function of w. Using, the geometric definitions as shown in Figure (15) and (16). The quantities a, b, and x are calculated using the law of cosines:

$$(R - w)^2 = 2x^2 - 2x^2 cos(a) \tag{48}$$

$$(R + w)^2 = 2x^2 - 2x^2 cos(b) \tag{49}$$

and using the fact that the sum of all angle around the center point of the octagon must be 360^o

$$4a + 4b = 2\pi \Rightarrow a + b = \frac{\pi}{2} \tag{50}$$

The three Equations (48), (49) and (50) above are solved simultaneously to to yield a, b, and x. The physically meaningful positive roots are selected. Adjacent (bonded) atoms have separation,

$$r_{12} = r_{34} = r_{56} = r_{78} = R - w \tag{51}$$

$$r_{23} = r_{45} = r_{67} = r_{18} = R + w \tag{52}$$

The second-nearest neighbor separation is determined using the law of cosines as,

$$r_{13} = r_{24} = ... = \sqrt{2x^2 - 2x^2 cos(\pi/2)}.x = \sqrt{2}.x \tag{53}$$

There are two types of third-nearest neighbor interactions. The law of cosines is used in the definition of both.

$$r_{14} = r_{36} = ... = \sqrt{2x^2 - 2x^2 cos(2a + b)} \tag{54}$$

$$r_{25} = r_{47} = ... = \sqrt{2x^2 - 2x^2 cos(a + 2b)} \tag{55}$$

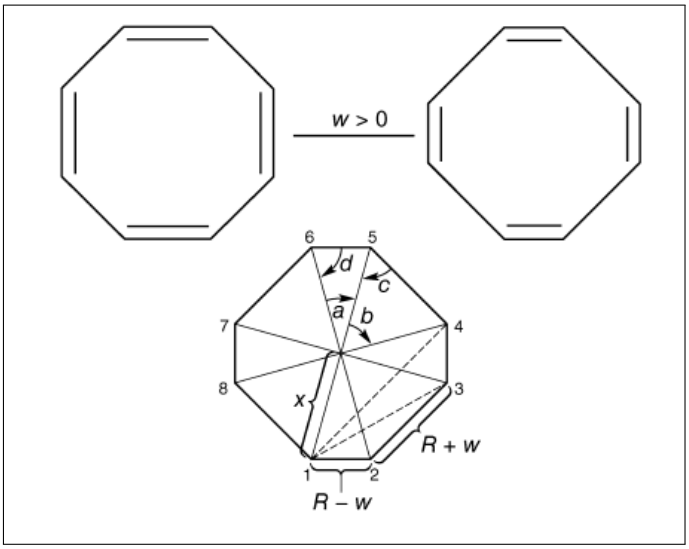

Fig. 15. Diagrammatic representation of the distortion parameter w and the structure of COTE. For w=0, COTE is a perfect octagon but as w increases the structure develops alternating short and long bonds, which can be characterized by the variable a, b, c, d, and x. These can be then used to determine the overlap between orbitals as shown in Equation (47).The Figure was obtained from Ref. [1]

The Equations (51), (52), (53), (54) and (55) are used to determine all of the atomic distances in the COTE molecule. A slight modification of these equations as described in [1] can be used to determine the atomic distances as a function of distortion parameter w for benzene as well.

We then use Equation (5) to determine the corresponding **S**-matrix elements, that is, the overlap integrals. To determine the **H** matrix we use the following approximation:

$$H_{ii} = -\mathbf{VOIE}(\chi_i) \tag{56}$$

$$H_{ij} = 0.875 \times S_{ij}(H_{ii} + H_{jj}) \tag{57}$$

where "VOIE" denotes "valence orbital ionization energy", that is, the ionization energy of an election in a χ_i orbital on an isolated atom of the corresponding element and is equal to 3.396 hartree = 10.77 eV for a carbon $2p$ electron. The off-diagonal elements of **H** is given by (57).

The above steps convert the Schrödinger equation to the secular form of the Equation (1). Solving these we get the molecular orbital energies according to HT. The computational algorithm used is discussed in Algorithm Table (1). This was implemented in C++.

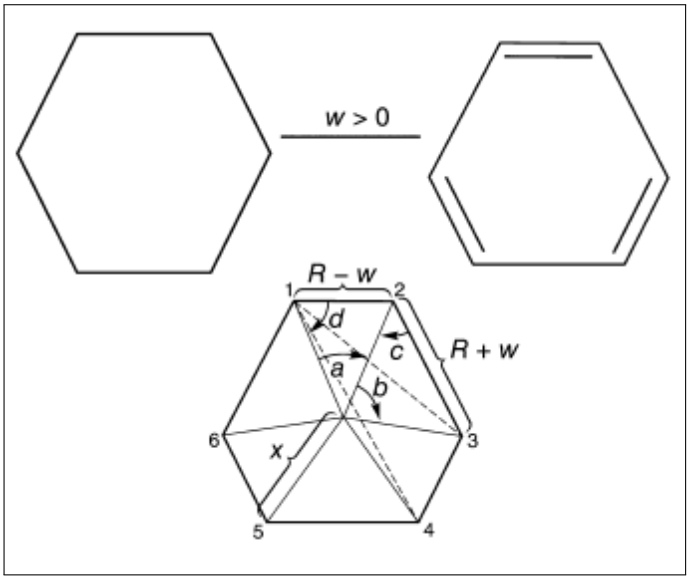

Fig. 16. Diagrammatic representation of the distortion parameter w and the structure of benzene. For w=0, benzene is a perfect hexagon but as w increases the structure develops alternating short and long bonds, which can be characterized by the variable a, b, c, d, and x. These can be then used to determine the overlap between orbitals as shown in Equation (47). The Figure was obtained from Ref. [1]

Algorithm 1. Steps

1: Set R, ζ and Z^{eff}.
2: Set w (the bond length variation)
3: Equations (48), (49) and (50) are are solved simultaneously for a, b, and x.
4: All of the inter atomic distances are calculated with Equations (51), (52), (53), (54), and (55).
5: All of the S-matrix elements are calculated with Equation (5)
6: All of the diagonal H-matrix elements are set with Equation (56) and (57).
7: All of the off-diagonal H-matrix elements are calculated with Equation (1).
8: Equation (3) is solved for the molecular orbital energies and the lowest four roots selected.
9: The total electronic energy is calculated with Equation (43) by placing the 8 electrons in the four lowest energy orbitals (6 in case of benzene).
10: The core-core repulsion energy is calculated with Equation (45).
11: The ground-state energy is calculated with Equation (46).
12: Steps 2-11 are repeated to generate a set of points describing the variation in the ground-state energy as a function of the distortion parameter w.

Steps for Calculations

A C++ code was developed to solve the above equations, the steps for which is given the algorithm Table (1).

The Jahn-Teller Effect in Action !

The procedure was implemented for COTE and benzene, the plot of those results are shown in the plots that follow. Each of the figures carry a detailed description of the results obtained.

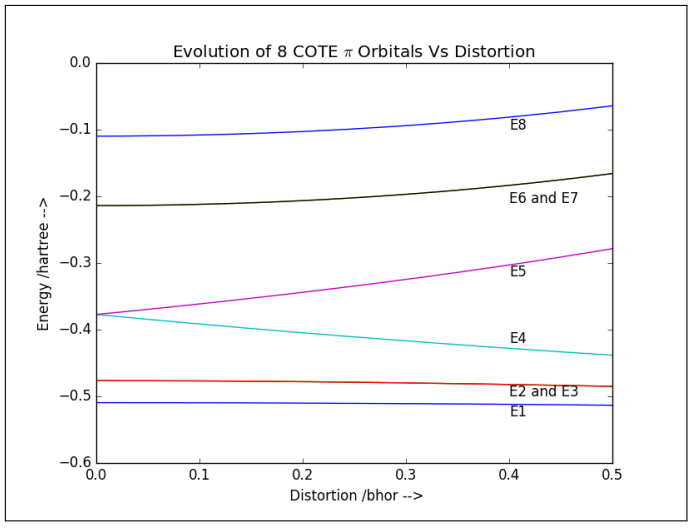

Fig. 17. Evolution of 8 COTE π orbital energies with the distortion parameter w. The π-orbital structure of COTE has 8 electrons, so the degenerate level at w = 0 is half-filled. Note that with increasing w the HOMO which was earlier degenerate is now split. This shows that on distortion all the electrons fill up the lower energy orbitals and the net result is a net decrease in energy. This is the Jahn-Teller distortion.

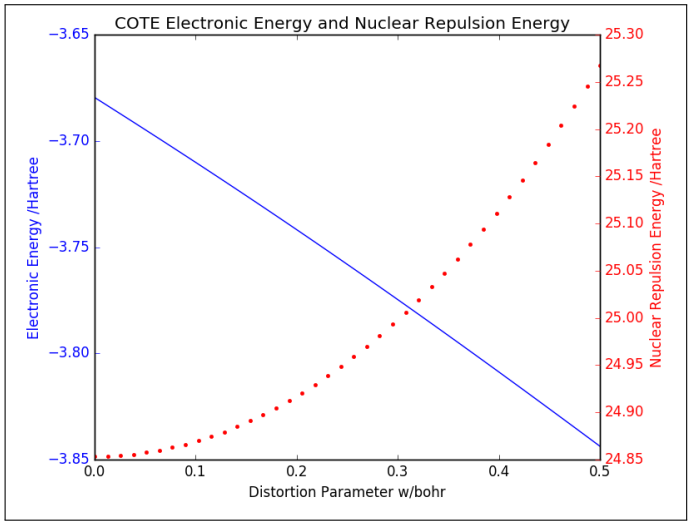

Fig. 18. This figure shows how the electronic energy and the core-core repulsion energy varies as a function of the distortion parameter w for COTE. Initially as w increases, the electronic energy decreases faster than the nuclear repulsion energy increases, so the ground-state energy decreases with increasing w, but at larger values of$w$, the nuclear repulsion energy increases more rapidly and the ground-state energy begins to increase with increasing w. This competition between terms leads to a minimum at w >0 and results in distortion of the bonds.

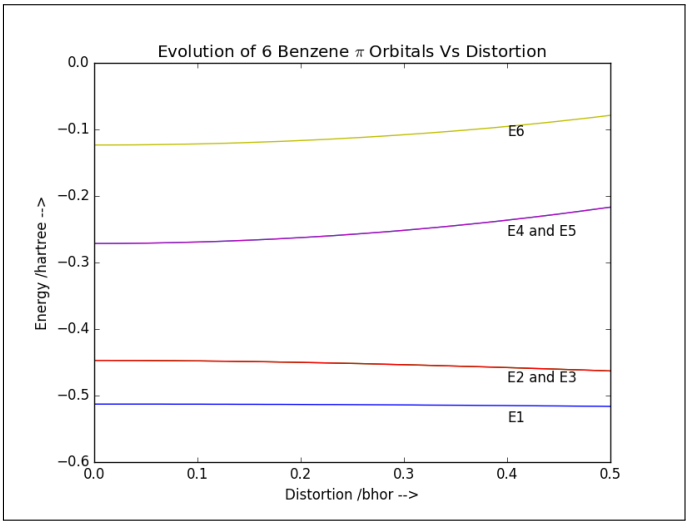

Fig. 20. Evolution of 6 benzene π orbital energies with the distortion parameter w. E2 and E3 are degenerate and so are E3 and E4. There is no splitting upon distortion.

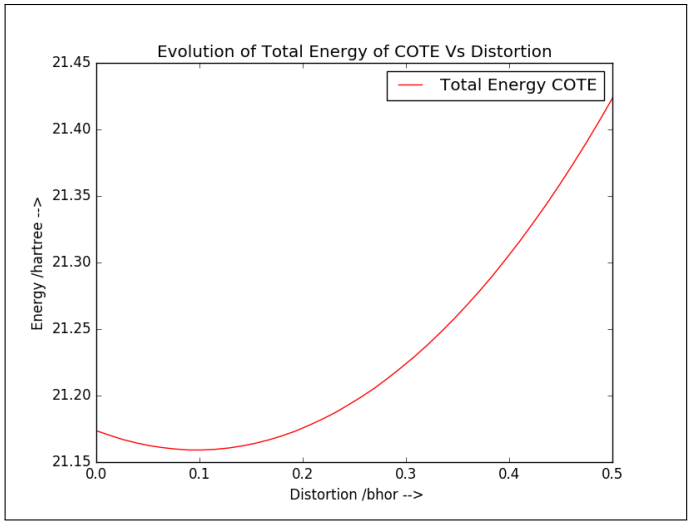

Fig. 19. Evolution of total energy of COTE as a function of the distortion parameter w. The minimum of the energy occurs for w >0. This predicts that COTE will undergo distortion from a perfect octagon to a structure with alternating short and long bonds, as is observed experimentally. This can be assumed to be the net resultant of the two curves in the Figure (18)

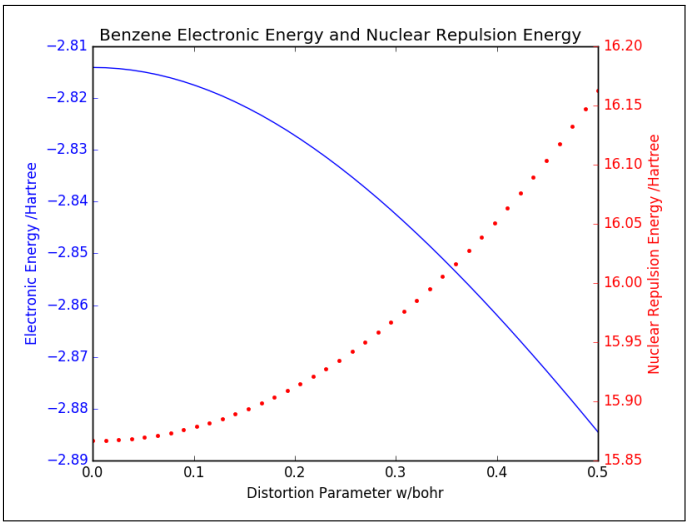

Fig. 21. This figure shows how the electronic energy and the core-core repulsion energy varies as a function of the distortion parameter w for benzene. We observe that electronic energy decrease at a slightly lower rate than the core-core repulsion energy increases as a function of w. Thus, the ground state energy keeps on increasing and the minima is at w=0, and hence we observe no distortion.

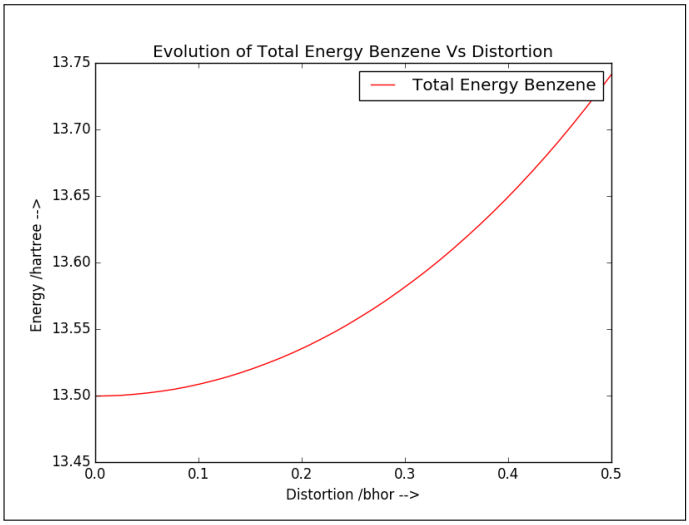

Fig. 22. Evolution of total energy of benzene as a function of w. This can be assumed to be the net resultant of the two curves in the Figure (21). This shows that the minimum of the energy is at w=0 and hence, Jahn-Teller distortion is not seen in case of benzene.

Peierls Distortion

A major break through in the area of conducting plastics was the discovery that polyacetylene, which is an insulator could be made highly conducting by exposing it to oxidizing (p-type doping $I_2, Br_2, FeCl_3$) or reducing agents(n-type doping). The structure of ployacetylene is shown in Figure (1), it is a long chain of CH groups, each possessing an unpaired electron, which can be looked at as a one-dimensional metal where each metal atom is replaced by an CH radicals. Since there is only one unpaired electron per CH group, a half-filled band is obtained so metallic conductivity is possible.

In reality, polyacetylene is characterized by alternating succession of short (double) and long (single) bonds. This behavior results form the Peierel's instability, which states that if a system with a given symmetry has a top occupied electronic orbital that is degenerate, then this orbital will interact with a vibrational mode that has symmetry lower than that of the original system, causing it to distort from the original configuration and thus splitting the degeneracy, which results in the appearance of a state of lower energy. This principle is also known as the Jahn-Teller effect. This distortion causes the degeneracy at the edge of the Brillouin zone to disappear and thereby lowering the Fermi level. Since, there is an energy gap at the Fermi level, the material ceases to be a conductor and instead becomes an insulator.

This distortion results in the appearance of two minima on the potential energy surface characterizing polyacetylene. These two minima correspond to two alternative crystal lattices which differ by the way the short and long bonds alternate in the crystal lattice. This is shown in Figure (23). In lattice I, the distance between the lattice points 1-2, 3-4 and 5-6 are shorter as compared to the distance between 2-3 and 4-5. In lattice II, distance between 2-3 and 4-5 is shorter than 1-2, 3-4 and 5-6. In this case, of *trans*-polyacetylene, these two alternative lattices are isoenergetic or degenerate. In Figure (24) we show that the lattice with identical distances between the lattice points is found at the maxima of the potential energy curve.

Similarly, in the case of *cis*-polyacetylene, Peierls distortion will cause the lattice with equal bond lengths Figure (25) (a) to distort to a lattice with alternating short and long bond-length Figure (25) (b) and (b). It can also exits in two lattices which differ from each other through the presence of the short or double bonds at different lattice points. In contrast to *trans*-polyacetylene, these two lattices are not iso-energetic. Figure (26) shows the energy configuration/plot of the two lattices along with the lattice with equal bond length which is at the energy maxima. The lattice showen in Figure (25) (b) has more efficient conjugation and is hence at a lower energy as shown in Figure (26).

The SSH model for this polyacetylene was computationally implemented in C++ and a plot of total energy and the π electron energy as a function of bond length alternation was obtained which is shown in Figure (27). As explained, we observe two minima on the potential energy surface characterizing polyacetylene. The π electron energy decrease as change in bond length affects the resonance integral.

The Hamiltonian used is :

$$\mathbf{H}(k;\Delta) = \begin{bmatrix} 0 & -1-\Delta \\ 0 & 0 \end{bmatrix} e^{-ik} + \begin{bmatrix} 0 & -1+\Delta \\ -1+\Delta & 0 \end{bmatrix} + \begin{bmatrix} 0 & 0 \\ -1-\Delta & 0 \end{bmatrix} + e^{ik} \tag{58}$$

The change in total energy per unit cell of polyacetylene is give as :

$$E(\Delta) = \frac{1}{K}\sum_{k=0}^{K} e_1(k;\Delta) + \frac{1}{2}k(\Delta^2 + \Delta^2) \tag{59}$$

Where K is the wavevectors that is sampled in the first Brillouin zone and e_1 is the valence band energy.

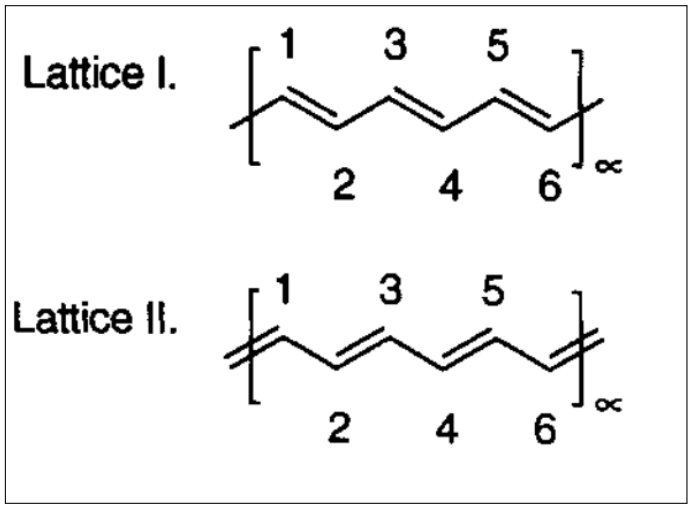

Fig. 23. Lattice structures in which *trans*-polyacetylene can exists.

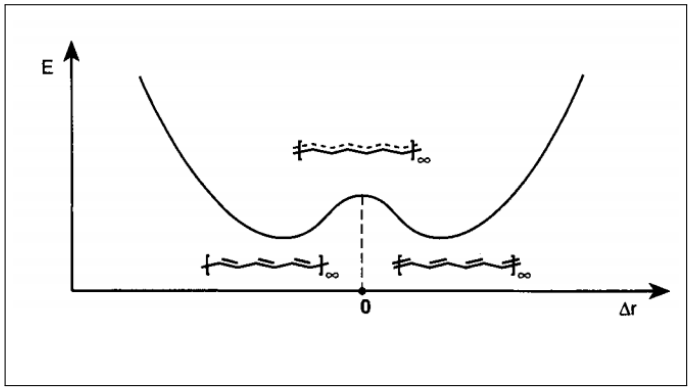

Fig. 24. Potential energy curve of *trans*-polyacetylene showing the energies of the two lattice configurations as a result of the Peierl's distortion.

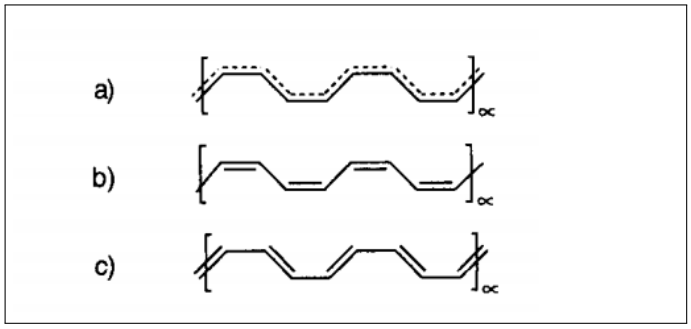

Fig. 25. Lattice structures in which *cis*-polyacetylene can exists.

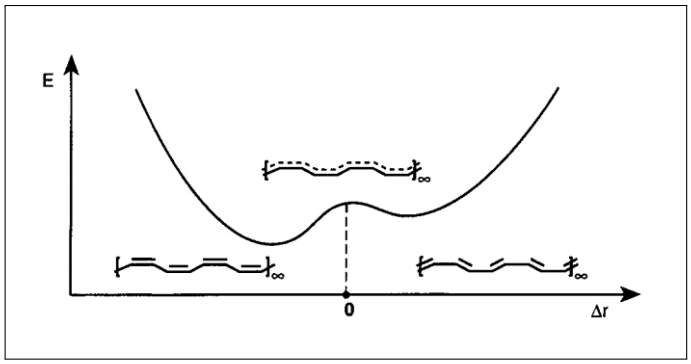

Fig. 26. Potential energy curve of *cis*-polyacetylene showing the energies of the two lattice configurations as a result of the Peierl's distortion. Note that the two lattice are not isoenergetic as was the case in *trans*-polyacetylene

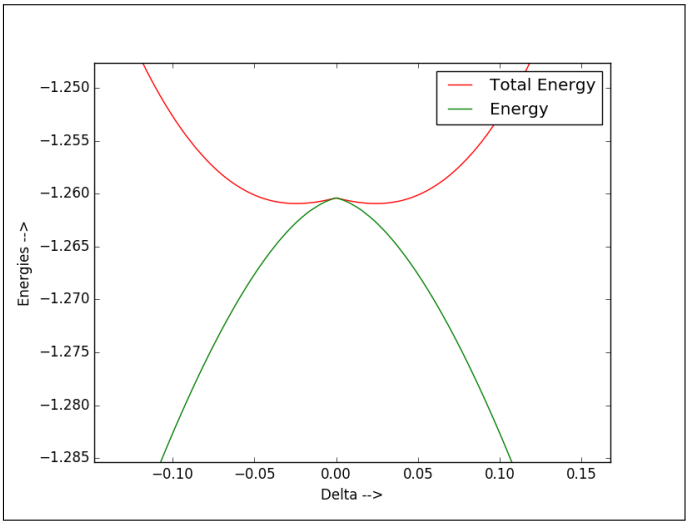

Fig. 27. Plot of the total energy and the π electron energy as a function of bond length alternation. We observe two minima on the potential energy surface characterizing polyacetylene.

FUNDING INFORMATION

Graduate Teaching Assistantship by the Chemistry Department at the University of Illinois at Urbana-Champaign (UIUC). Computational resources were provided by the Hirata Lab, UIUC.

ACKNOWLEDGMENTS

Many thanks to Prof. So Hirata for his guidance and patience while teaching this course

REFERENCES

1. Karl, S. *J. Chem. Educ.*, 2013, 90 (4), 463–469.
2. Senn, P. *J. Chem. Educ.*, 1992, 69 (10), 819-821.
3. Bacci, M. *J. Chem. Educ.*, 1982, 59 (10), 816-818.
4. https://en.wikipedia.org/wiki/H%C3%BCckelmethod accessed on March 23rd, 2017.
5. https://ocw.mit.edu/courses/chemistry/5-61-physical-chemistry-fall-2007/lecture-notes/lecture31.pdf accessed on March 23rd, 2017.
6. Levine, I. N. *Quantum Chemistry*, 5th ed.; Prentice Hall:: Upper Saddle River, NJ, 1999; p 739.
7. Szabo, A. , Ostlund N. S. *Modern Quantum Chemistry: Introduction to Advanced Electronic Structure Theory*, Dover Books on Chemistry::31 East 2nd Street, Mineola, NY 11501-3852
8. Asboth, J, K., Oroszlany, L., Palyi, A., A Short Course on Topological Insulators Band-structure topology and edge states in one and two dimensions. Lecture Notes, Springer.
9. Lindner, D. P. R., Sekiya, H.,Beyl, D. P. B., Müller-Dethlefs, K., *Angewandte Chemie*, 1993, 32 (4), 603-606.